PROCEEDINGS OF THE 2ND ASIA-PACIFIC CONFERENCE ON SHOCK & IMPACT LOADS ON STRUCTURES

Melbourne, Australia
25 - 27 November 1997

Editor
T S Lok
Nanyang Technological University
Singapore

ISBN: 981-00-8906-6

organised by:
CI-Premier Conference Organisation
Singapore

in conjunction with:
Kohway Enterprise Australia Pty Ltd
Australia

with the support of:
- DSTO - Ship Structures and Materials Division, Australia
- Japan Society of Civil Engineers (The Impact Problem Research Committee), Japan
- Monash University (Department of Civil Engineering), Australia
- The Hokkaido Development Bureau, Japan

conference official carrier

Fracture Analysis of Seismic Bridge Restrainers under Impact Loads

F Nagashima, Tokyo Metropolitan University, Japan
M Minagawa, Musashi Institute of Technology, Japan
Y Sonoda, National Defense Academy, Japan
N Ishikawa, National Defense Academy, Japan

ABSTRACT

This paper focuses on the seismic performance of bridge connecting plates and analytically examine the impact behavior and energy absorbability to impulsive seismic loads. First, we evaluate the impulsive loading speed for the plates by analyzing nonlinear dynamic response of elevated bridges to some recorded waves during the Kobe Earthquake in 1995. The falling body problem of the complete bridge girder model with seismic connecting plates in the gravity field is also discussed. Secondly we analyze impact behavior of the bridge connecting plates using three dimensional finite element code introducing the stress-strain relationship obtained from tensile failure tests of steel rods.

Throughout the summary of these analytical studies, the appropriate values of rate-dependent material parameters of connecting plates used for fracture analyses were obtained.

1. INTRODUCTION

The seismic bridge restrainer systems, the bridge connecting plates connecting each of the adjacent girders or connecting a girder to an abutment, movement-limiters attached to a bearing and a wide seat abutment or a column bent, are used to prevent the superstructures from unseating [1]. In Japan, these seismic systems have been used since the Showa Ohashi bridge fell off during the Niigata Earthquake (June 16, 1964; M7.5). During the Kobe Earthquake (January 17, 1995; M7.2), however, many bridges, such as curved and the skew bridges, the side span of the main Nishinomiyako bridge and the single bent and simple supported bridge, fell off their seat column bent.

There have been no satisfactory methods developed for designing the strength and stiffness of restrainers to be placed across movement joints [2]. Since the Kobe Earthquake, the researches on developing bridge-unseating preventing devices have had important considerations.

The design load of connecting plates for a road bridge greatly depends on the design method used and may be either: (1) $\sqrt{2}$ times a half of the dead load (Rd) of a girder: This design load is based on the assumption that a girder end falls off a pier top if the lateral spreading due to liquefaction moves and inclines the pier or causes the pier to hit another as occurred during the Kobe Earthquake. (2) safety factor (γ; γ =1 to 4) $\times$ the design seismic coefficient (Kh; Kh $\fallingdotseq$ 0.2 to 0.3) $\times$ girder weight (2Rd) $\fallingdotseq$ 0.4 γ Rd$\sim$0.6 γ Rd: This design load is based on the assumption that a girder end dose not fall off a pier top during an earthquake.

The other important factor to be considered is whether or not the coefficient of extra intensity to the allowable stress is appropriate. These subjects should be approached from the following two viewpoints: (i) Trilateral effects of the structures that prevent bridge fall, such as drift limiting devices, seating length, and bridge-unseating preventing devices, (ii) Shock on the girder connecting device in the worst case scenario that the bridge should fall.

The purpose of the present study was to clarify the shock response characteristics of seismic connecting plates used as a bridge-fall preventing device and to obtain some fundamental reference data on the design forces by performing dynamic response analyses in the gravity field and high-speed fracture analysis .

2. OVERVIEW OF THE DAMAGES OF BRIDGE CONNECTING DEVICES

Every damage modes of the bridge connecting devices considered to be possible to occur, except for the destruction of stiffened part of web plate was observed during the Kobe Earthquake (Photo1 - Photo 5) [3, 4].

First, when a strong earthquake occurs, initially movement-limiters of movable bearings are destroyed. Next, considering the pier to be rigidly enough to withstand the shock, the impulsive forces, produce additional effects to the connecting device. At this instant, the applied forces exceed the yield strength (proof stress) and cause the coupling pin to fall off (Photo 1). Then the bridge connecting plate , anchorage and web plate is torn off. Moreover, the relative displacement of the pier exceeding the allowable seating length causing the structure to fall down.

Bridge-unseating preventing device works in a degree effectively. In Photo 2, there is some evidence of movement of the device along all the clearance of the pin hole, and some traces of plastic deformation are observed at the tip of the connecting plate. In Photo 3, due to excessive application of horizontal forces, the tip of the connecting plate was torn off. Also, it is noted that the connecting device reduced the effect of the earthquake impact along the transverse direction as shown in Photo 4.

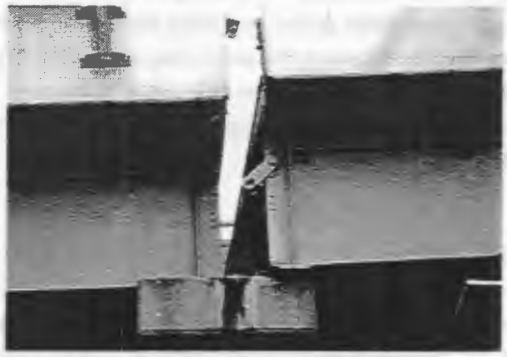

Photo 1 Falling off of coupling pins

Photo 2 Plastic deformation and scratched mark

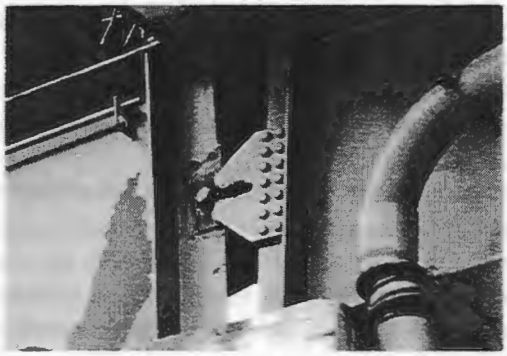

Photo 3 Destruction of the connecting plate

Photo 4 Tearing off; Anchorage of the connecting device

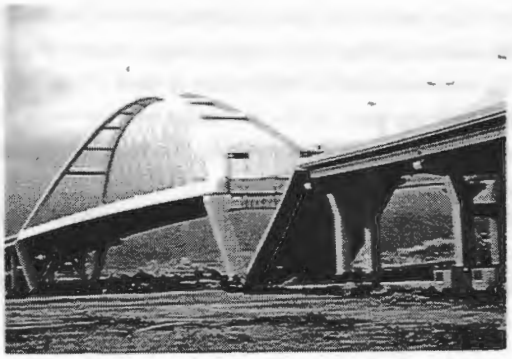

Photo 5 Unseating, side span of the Nishinomiyako bridge

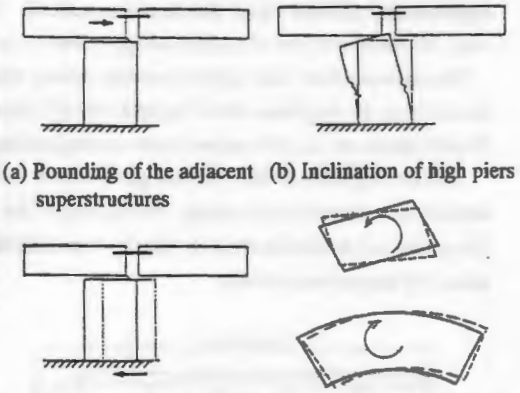

Fig. 2.1 Bridge unseating modes

There are also some incidences that bridge unseating occurred even though the span between the piers didn't open so much (Photo 5). As shown in Figure 2.1, following failure modes were also observed; (a) Bridge unseating caused by the pounding of adjacent superstructures with different natural frequencies or accumulated side-sway displacement, (b) Bridge unseating caused by the inclination of high piers, (c) Bridge unseating caused by the pier movement due to ground liquefaction or lateral flow, and (d) Bridge unseating caused by transverse or rotational motion of the girder in the case of skew bridges [5] or curve bridges.

Bridge connecting devises were damaged on some parts of web plates, pins, connecting plates and anchorages. To make a rational design, we should assign adequate strengths to these parts. And we should develop a detail of connecting plates with high capacity of energy absorption. Also, we should establish the ultimate design method of the connecting plates and structural analysis up to failure should be considered in the near future.

3. NONLINEAR DYNAMIC ANALYSIS OF BRIDGES

To evaluate the maximum relative displacement and maximum relative velocity of the girders, a nonlinear dynamic response analysis was performed on the pier-superstructure coupling system. Since a lot of isolated bridge systems are being considered for construction after Kobe Earthquake, isolation type bridges (LRB; Lead Rubber Bearing), as well as bearing type bridges were investigated for this research.

The bridge model shown in Figure 3.1 (a), (b) was a five-span continuous girder bridge with equal span of 50 m. The height of the piers were 10 m and 20 m respectively. Two different types of bridges of a steel bridge (here after called the steel model) and reinforced concrete bridge (here after called the RC model) were analyzed. The superstructures of these bridges were modeled as steel box girders with a dead load of 3,250 tf (ton-force). Both the steel and RC models were of T-shape piers with rectangular cross-section. The moment and curvature relationships of the piers, M-ϕ curves as shown in Figure 3.1 (c), were calculated by the method of dissection.

Utilizing these M-ϕ curves dynamic response analyses were performed and the maximum response displacement and maximum response velocity were investigated. The analytical model is of bending-shear model consisting mainly of beam, mass and spring.

In Table 3.1, the values of the maximum response displacement and maximum response velocity are tabulated. Input ground acceleration waves are Standard Wave I, II, III, and strong ground motion records observed by Japan Meteorological Agency [Kobe] and Japan Railway [Takatori station] during the Kobe Earthquake. The notation of SS and PT in this table means the position of nodal point corresponding to the Superstructure and the Pier Top respec-

tively. It is noted that piers with height of 10 m subjected to any input wave yield the same amount of displacement regardless the material which the piers were made of. The maximum value of the response displacement was 67 cm. Also, the girder and pier of isolated bridge system yield the maximum relative displacement of about 40 cm.

The superstructure yields greater response velocity than the pier top does. For the steel bridge with pier height of 10 m and 20 m, the response velocity ranged 100-187 cm/sec or 139-234 cm/sec, respectively. For RC bridge, it ranges 95-183 cm/sec or 112-190 cm/sec for the corresponding cases.

It is also significant that when the girders move in inverse phase, about twice the displacement and the velocity should be considered in the design. On the base of this assumption, it can be concluded that maximum relative displacement and maximum relative velocity to be considered in designing the connecting plates is about 100 cm and about 350 cm/sec respectively.

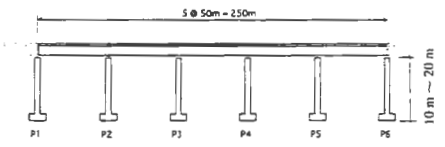

(a) Elevated continuous girder bridge

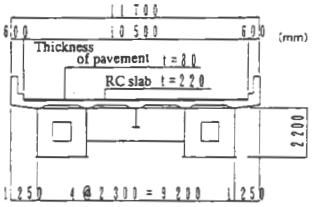

← (b) Superstructure (Steel box girder, 3,200 tf)

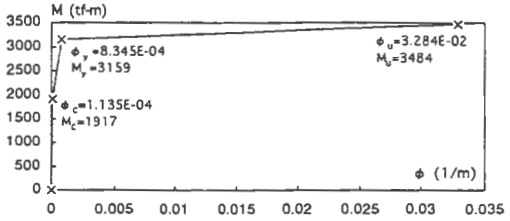

(c) M - ϕ relationship (RC bridge, pier height; 10 m)

Fig. 3.1 Five - span continuous girder bridge model

Table 3.1 Maximum response displacement and Maximum response velocity

(disp.; cm, vel.; cm / sec)			SW(Ⅰ) disp.	SW(Ⅰ) vel.	SW(Ⅱ) disp.	SW(Ⅱ) vel.	SW(Ⅲ) disp.	SW(Ⅲ) vel.	Kobe JMA disp.	Kobe JMA vel.	JR Takatori disp.	JR Takatori vel.
10m-Steel	Isolation	SS	26.9	100.2	31.9	139.6	29.8	121.2	23.7	144.0	41.8	187.1
		PT	1.8	8.7	2.1	11.4	2.0	11.0	1.7	9.0	2.7	15.2
	Bearing	SS=PT	2.6	29.3	2.8	44.3	3.5	54.8	7.3	84.2	5.6	76.2
20m-Steel	Isolation	SS	41.3	139.0	52.8	172.2	65.9	209.6	31.2	145.5	66.9	221.5
		PT	18.8	67.1	24.2	83.3	30.7	101.7	13.7	69.2	31.2	104.8
	Bearing	SS=PT	35.3	141.6	45.4	177.0	52.4	184.4	38.3	208.5	62.4	234.2
10m-RC	Isolation	SS	26.1	95.4	30.4	134.8	29.1	117.1	22.9	140.5	39.9	183.2
		PT	1.1	9.5	1.5	10.6	1.3	9.8	1.1	11.4	2.9	21.8
	Bearing	SS=PT	1.3	12.8	1.7	21.4	2.0	25.6	7.4	39.9	3.5	40.4
20m-RC	Isolation	SS	30.9	111.8	34.7	149.4	35.8	130.5	26.6	142.7	45.8	190.0
		PT	7.7	35.5	9.0	40.7	10.7	45.9	9.8	83.9	11.1	85.9
	Bearing	SS=PT	11.5	58.9	12.9	68.5	13.2	68.0	19.3	146.7	27.3	108.5

4. IMPACT BEHAVIOR OF BRIDGE CONNECTING PLATES

Shock response analyses were performed in order to examine impact behavior that a bridge unseating may produce on a girder connecting device. Concerning these kinds of problems as the problems in the gravitational field, three dimensional nonlinear impact response analyses were numerically performed utilizing the analytical model as shown in Figure 4.1 and Table 4.1. It takes about 28 hours for calculating one case with Sun Spark Station 20. Analytical results confirmed the facts mentioned below.

Out-of-plane plastic deformation of connecting plates (Fig. 4.2), which was one of the typical failure modes observed in girder bridges damaged by the Kobe Earthquake, necessarily occurs by the action of longitudinal severe loads. Mainly because of the existence of the clearance between a connection plate and stiffening plates, which are

usually set for preventing coupling pins from shearing failure, coupling pins seem to be pulled by the connection plate acting like a bottle opener.

In figure 4.3, time history of tensile force applying to one of the pair of connecting plates. The maximum tensile force was found to be f_{max} = 72.7 tf = 2.63 $\sqrt{2}$ (Rd/2), and equivalent impact coefficient would be Ie = 2.63. When the ratio (σ_y / σ_a) of the yield stress to the maximum stress and the ration (σ_m / σ_a) to the allowable stress are assumed to be 1.7 and 2.9 respectively, the plate still remains in the state of yielding [1.7 $\sqrt{2}$(Rd/2) < 2.63 $\sqrt{2}$(Rd/2) < 2.9$\sqrt{2}$(Rd/2)], and the internal stress is in the range of flow stress. Therefore, the design force of connection plates under consideration of suspending states of bridge girders should be $\sqrt{2}$ Rd per a girder at least in the working stress design.

The velocity of the forces acting to the connection plates was 267 cm/sec. The loading velocity seems to result in strain rate of 20 - 25 sec^{-1} that should be considered strain-rate effects for the material properties. More detailed description of the strain-rate effects are found in the next section about impact fracture analyses.

Table 4.1

Span: 30.0 m
Girder depth : 1.7 m
Dead load (Rd; per a girder): 39.09 t f
Number of elements: 1,780 (solid) + 372 (shell)

M: Movement joint, F: Fixed joint

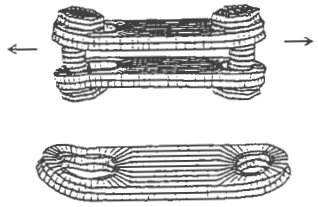

Fig. 4.2 Out-of-plane plastic deformation of the connecting plate (analyzed)

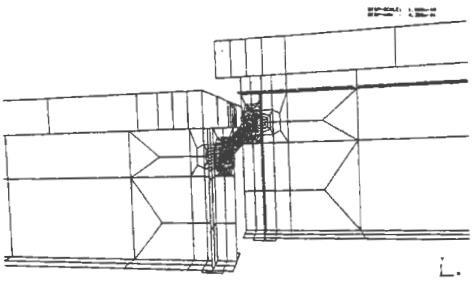

Fig. 4.1 Analytical model of the superstructures and connecting device

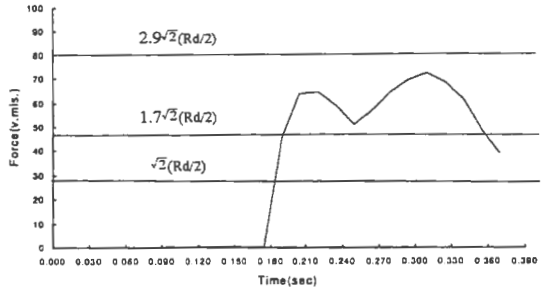

Fig. 4.3 Time history of tensile force applying to one of the pair of the plates (analyzed)

5. IMPACT FRACTURE ANALYSIS OF CONNECTING PLATES

Against extremely severe earthquakes like the Kobe Earthquake, which may not occur in the life of structures, secondary members or attached members as connection facility should serve to maintain the minimum functional requirement of bridges which is to let vehicles pass after emergency treatment. Allowable damage design method is based on the philosophy mentioned above. To establish this type of design method for any structures, failure behavior of structural members should be clarified.

In this section, single-hole type connecting plates (as shown in photo 2 and 3) subjected to impact loads were investigated with three dimensional nonlinear impact analyses and compared with experimental results. In the comparisons, the effects of strain rate on stress-strain relationship are considered.

We first carried out static loading tests and high speed loading tests with the loading speed of 400 cm/sec of single hole-type connecting plates. Materials used for the connecting plates and the coupling pins were SS400 and S35C, respectively. The experimental apparatus for the high speed loading tests is given in Figure 5.1. The loading test was performed by pushing down the loading plate that was linked with the test specimen (connecting plate).

In order to simulate the failure behavior of connection plates under relatively high strain rate and to generalize the behavior, three dimensional elastoplastic fracture analyses were performed with the finite element code LS-DYNA3D. In the analyses isotropic elastoplastic solid (with failure) elements were used.

The failure was judged with one of the following criteria [6];

1. Effective plastic strain exceeds the maximum plastic strain limit;

$$\varepsilon^{P}_{eff} > \varepsilon^{P}_{\max}, \quad ; \varepsilon^{P}_{eff} = \int_0^t (\frac{2}{3}\dot{\varepsilon}^{P}_{ij}\dot{\varepsilon}^{P}_{ij})^{1/2} dt \quad \text{..... (5.1)}$$

where ε^{P}_{eff} is the effective plastic strain, $\varepsilon^{P}_{\max}$ is the maximum plastic strain, and $\dot{\varepsilon}^{P}_{ij}$ is the plastic strain rate.

2. Compressive stress exceeds the maximum compressive stress, then

$$p^{n+1} < p_{\min}, \quad ; p^{n+1} = K(\frac{1}{V^{n+1}} - 1) \quad \text{..... (5.2)}$$

where p^{n+1} is the compressive stress at the n+1 calculation step, $p_{\min}$ is the maximum compressive stress, K is the bulk modulus of elasticity, and V^{n+1} is the volume at the n+1 calculation step. In case the one of the criteria is satisfied in any finite element, the element is removed from the following calculation step. Therefore crack propagation can be evaluated through the calculation.

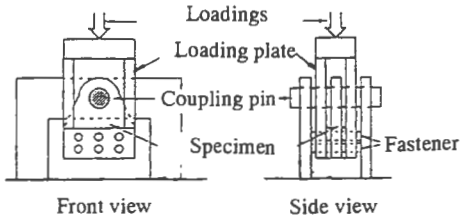

Fig. 5.1 Schematic for the high-speed test apparatus

A steel bar specimen made of SS400 which is the same as the connecting plate was subjected to tensile failure test in order to validate the failure criteria. In this experiment, basing from the stress-strain relationship, the properties corresponding to the analysis of the bridge connecting system were obtained. The stress-strain relationship is shown in Figure 5.2 comparing the results of the experiment and the results obtained from the analysis using failure model as shown in Figure 5.3.

Each material parameter used in this analysis is shown in Table 5.1. The Young's modulus, shear modulus and mass density was taken at general values.

The effect of loading speed is introduced in the analyses by changing the material properties of each material depending on the strain rate according to the ref. [7]. The ratio of the yield stress under high speed loading to the stress under static loading is given by the following equation;

$$\Delta f_y = \frac{\sigma_{yd}}{\sigma_{ys}} = 1.202 + 0.040\log\dot{\varepsilon} \quad \text{..... (5.3)}$$

,where $\dot{\varepsilon}$ is strain rate. The ratio of the maximum stress under high speed loading to the stress under static loading is also given by the following equation;

$$\Delta f_u = \frac{\sigma_{ud}}{\sigma_{us}} = 1.172 + 0.037\log\dot{\varepsilon} \quad \text{..... (5.4)}$$

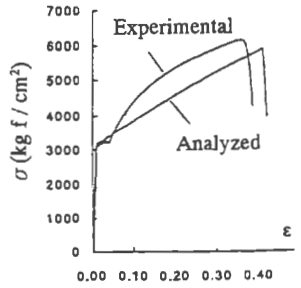

Fig. 5.2 Stress - strain relationship

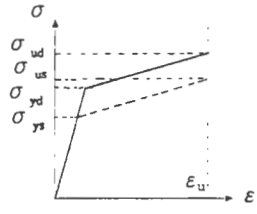

Fig. 5.4 Bilinear stress - strain curve model

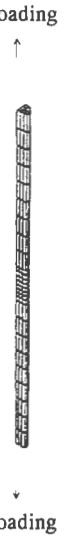

Fig. 5.3 Steel bar model (a quarter part)

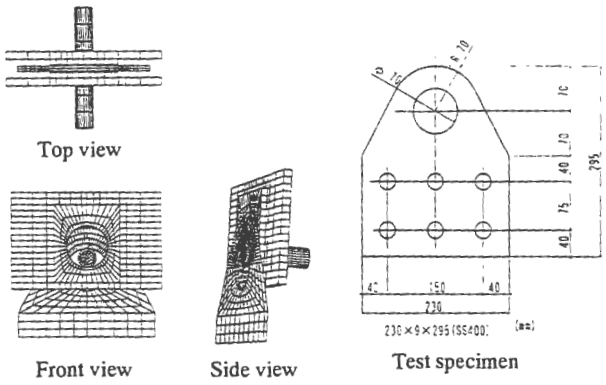

Fig. 5.5 bridge connecting plate model

Table 5.1

Young's modulus (kgf/cm²)	E :	2.10×10^{6}
Tangent modulus (kgf/cm²)	E_t:	8.20×10^{3}
Shear modulus (kgf/cm²)	G:	8.08×10^{5}
Yield stress (kgf/cm²)	σ_y:	3.10×10^{3}
Failure strain	ε_u:	3.85×10^{-1}
Mass density (kgf/cm³)	ρ :	8.01×10^{-6}

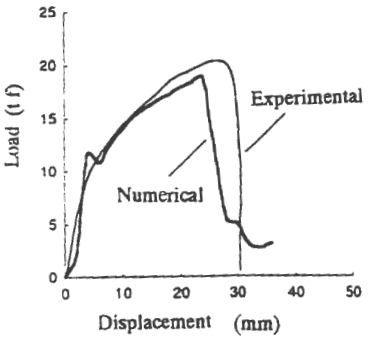

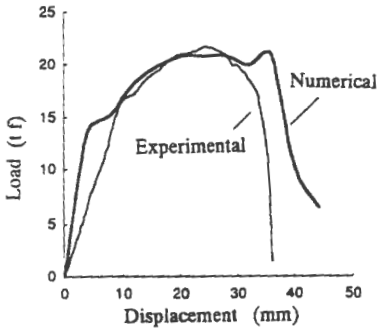

Fig. 5.7 Load-displacement relationship

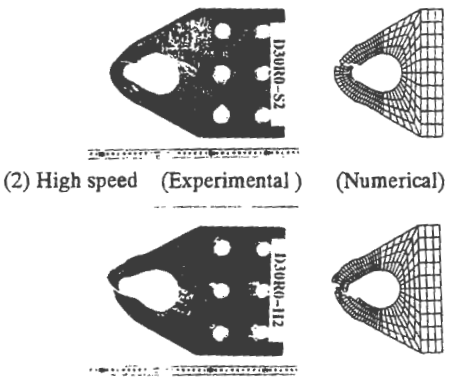

Fig. 5.6 Plastic deformation and fracture mode

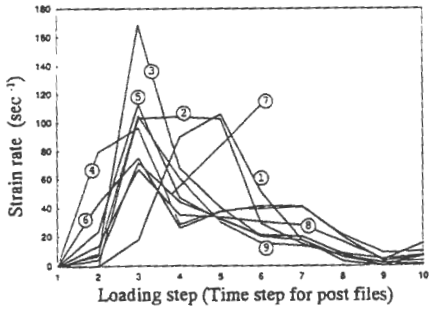

(a) Strain rates curves of the failure elements

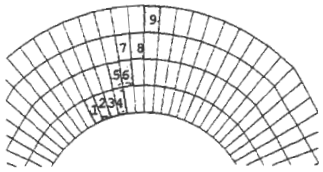

(b) Failure elements and element numbers

Fig. 5.8 Strain rate at each time step

The bridge connecting device model, as shown in Figure 5.5, was solved as the contact problem between the pin surface and the connecting- plate inner nodes.

The impact behavior of connection plates simulated with the analyses are compared with the experimental results in both cases of (1) the static loading and (2) the high speed loading and given in Figure 5.6 and 5.7.

In all the analyses, the simplest failure elements are used as mentioned above, and the average value of strain rate ($\dot{\varepsilon}$=44) is adopted to estimate material properties of the elements. Nevertheless, in both cases of the static loading and

dynamic loading, the load-displacement relationships obtained by the analyses closely simulated the relationships measured by the experiments. The failure mode observed in the experiments, including the position the failure crack initiates as well as the direction of the crack propagation, is coincident to the mode simulated by the analyses very well. It is clear that the loading rate affects the crack propagation direction and the shape of the failure shape.

In Figure 5.8(a), the change in strain rate are shown in selected time step of the analyses. The each number in the figure shows the element number shown in Figure 5.8(b). These elements are on the root of rack propagation. The failure occurred at the 11th time step. Even though the strain rate in some early loading steps (around the 3rd step) increased remarkably, the rate became slower just before the failure occur.

Although the average strain rate was used in this analysis, it is necessary to analyze the structure subjected to change in strain rate in every step operation and change in material parameter. But comparatively good results were obtained from this analysis considering a strain rate below 100 sec^{-1}.

6. CONCLUSIONS

The conclusions obtained from the present study are summarized as follows;

1. In the Kobe Earthquake of 1995, every damage mode were seen from bridge fallout restraining systems. Different varieties of ruptures or fractures were seen from girders specially those of skew bridges and curved bridges .
2. There have also been incidences that bridge-fall may occur even though the span between the piers didn't open so much. The unseating mode consisted of four types. Therefore, it is significant to consider suspended conditions as the ultimate design.
3. As the results of the earthquake response analysis, it is found that the loading speed to the seismic connecting plates will be 200-350 cm/sec.
4. Based from the fracture analysis model parameter of the bridge connecting plates, good numerical predictions were obtained when the tensile fracture test of the steel rod was numerically validated.
5. In the high-speed loading fracture analysis, the strain rate effect lead to good results although only a simple model (bilinear model of Takahashi's empirical formula) was used.
6. Throughout the summary of these analytical studies, the appropriate values of rate-dependent material parameters, yield stress, hardening modulus and failure strain, of connecting plates used for fracture analyses were obtained.

REFERENCES

[1] Japan Road Association, "Design Specifications of Highway Bridges - Part V Seismic Design", 1990.

[2] Prieestley, M. J. N., Seible F. and Calvi, G. M. "Seismic Design and Retrofit of Bridges", John Wiley & Sons, 1996.

[3] F. Nagashima and T. Mochizuki, "Damage Caused by the 1995 Great Hanshin-Awaji Earthquake to Transportation Systems and the Recovery of These Systems", Comprehensive Urban Studies, No. 61, pp.63-77, Dec., 1996.

[4] F. Nagashima, " Effects of Bridge Restrainers on the Seismic Performance in the Great Hanshin-Awaji Earthquak"e, Proc. of the 51st Annual Meeting of JSCE, I-A282, pp564-565, Sep., 1996.

[5] Earthquake Engineering Research Institute, " Northridge Earthquake January 17", Preliminary Reconnaissance Report, 1994.

[6] J. O. Hallquist," LS-Dyna3D Theoretical Manual", Livermore Software Technology Co., 1994.

[7] Y. Takahashi,"Fundamental Studies on Evaluating Method of Impact Performance of RC Beams and Composite Beams", Doctor's Thesis of Kyushu Univ., 1990.